Journal of Power Sources 269 (2014) 173–179

Contents lists available at ScienceDirect

Journal of Power Sources

journal homepage: www.elsevier.com/locate/jpowsour

Improving carbon dioxide yields and cell efficiencies for ethanol oxidation by potential scanning

Pasha Majidi, Peter G. Pickup*

Department of Chemistry, Memorial University, St. John's, Newfoundland A1B 3X7, Canada

HIGHLIGHTS

- Ethanol oxidation has been investigated under cycling conditions.
- This increases efficiency by increasing the yield of carbon dioxide.
- Higher temperatures and a PtRu catalyst increase efficiencies further.
- The efficiencies of direct ethanol fuel cells can be increased.

ARTICLE INFO

Article history:
Received 12 March 2014
Received in revised form
12 June 2014
Accepted 1 July 2014
Available online 9 July 2014

Keywords:
Ethanol
Oxidation
Fuel cell
Efficiency
Products

ABSTRACT

An ethanol electrolysis cell with aqueous ethanol supplied to the anode and nitrogen at the cathode has been operated under potential cycling conditions in order to increase the yield of carbon dioxide and thereby increase cell efficiency relative to operation at a fixed potential. At ambient temperature, faradaic yields of CO_2 as high as 26% have been achieved, while only transient CO_2 production was observed at constant potential. Yields increased substantially at higher temperatures, with maximum values at Pt anodes reaching 45% at constant potential and 65% under potential cycling conditions. Use of a PtRu anode increased the cell efficiency by decreasing the anode potential, but this was offset by decreased CO_2 yields. Nonetheless, cycling increased the efficiency relative to constant potential. The maximum yields at PtRu and 80 °C were 13% at constant potential and 32% under potential cycling. The increased yields under cycling conditions have been attributed to periodic oxidative stripping of adsorbed CO, which occurs at lower potentials on PtRu than on Pt. These results will be important in the optimization of operating conditions for direct ethanol fuel cells and for the electrolysis of ethanol to produce clean hydrogen.

1. Introduction

With the heavy demand for sustainable fuel sources instead of fossil fuels, fuel cells employing alcohols are becoming very attractive [1–6]. In comparison to methanol, ethanol has important advantages but also presents much more difficult challenges. First and foremost, there is already a well-developed infrastructure for renewable production of ethanol, and it is less toxic than methanol. Furthermore, the energy density of ethanol (8.0 kWh kg^{-1}) is greater than that of methanol (6.0 kWh kg^{-1}) and closer to the energy density of gasoline (10 kWh kg^{-1}). Consequently, there is rapidly growing development of direct ethanol fuel cells (DEFCs) based on proton exchange membrane technology [4,6,7].

The main challenge in the development of DEFCs is that their efficiencies are very low relative to the theoretical value of 97% [2], and relative to efficiencies that can be achieved with hydrogen, methanol, and formic acid. The overall energy efficiency of a DEFC is determined by its electrochemical efficiency (theoretical efficiency *x* cell potential/reversible cell potential), the ethanol oxidation efficiency (i.e. the average number of electrons passed per molecule (n_{av}) relative to the maximum available ($n_{max} = 12$ for ethanol)), and the loss of ethanol to crossover [8]. The complete oxidation of ethanol involves the transfer of 12 electrons (Eq. (1)), while incomplete oxidation of ethanol to acetaldehyde ($n = 2$; Eq. (2)) or acetic acid ($n = 4$; Eq. (3)) will reduce the efficiency of the fuel cell considerably.

$$CH_3CH_2OH + 3H_2O \rightarrow 2CO_2 + 12e^- + 12H^+ \quad (1)$$

$$CH_3CH_2OH \rightarrow CH_3CHO + 2e^- + 2H^+ \quad (2)$$

* Corresponding author. Tel.: +1 709 864 8657; fax: +1 709 864 3702.
E-mail address: ppickup@mun.ca (P.G. Pickup).

http://dx.doi.org/10.1016/j.jpowsour.2014.07.002
0378-7753/

$$CH_3CH_2OH + H_2O \rightarrow CH_3CO_2H + 4e^- + 4H^+ \quad (3)$$

The electrochemical efficiency (voltage efficiency) is determined by the cell voltage, and so is strongly influenced by the activity of the anode catalyst. Much effort has therefore been applied to understanding the mechanism of the anodic oxidation of ethanol [7,9–13], and the development of more active electrocatalysts [7,14]. PtRu, PtSn, PtRuSn, and PtRuRh based catalysts have been found to be particularly active and many other combinations of Pt with other metals and oxides have shown high activity [14]. One if the key issues limiting the performance of the anode catalyst during ethanol oxidation is poisoning of the anode by strongly adsorbed CO and other intermediate (collectively referred to as CO_{ads} herein) on the catalyst surface. Thus, to increase the efficiency and performance of DEFCs, the formation of CO_{ads} should be inhibited and/or the catalyst should efficiently oxidize CO_{ads} to CO_2.

The ethanol oxidation efficiency (chemical efficiency; $n_{av}/12$) depends on the completeness of the ethanol oxidation reaction, and is determined by the weighted average faradaic yields ($\%_{product}$) of all of the products. If it is assumed that CH_3CHO, CH_3CO_2H, and CO_2 are the only products, n_{av} is given by Eq. (4) (note that one molecule of ethanol produces two molecules of CO_2).

$$n_{av} = (2x\%_{CH_3CHO} + 4x\%_{CH_3CO_2H} + 6x\%_{CO_2})/(\%_{CH_3CHO} + \%_{CH_3CO_2H} + \%_{CO_2}/2) \quad (4)$$

It is clear from this relationship that chemical efficiency can be greatly increased by increasing the yield of CO_2. This has been achieved mainly by increasing the operating temperature of the cell [15–21], which promotes cleavage of the C–C bond and has the added benefit of increasing the activity of the catalyst (increased voltage efficiency). However, operation of PEM type DEFCs is limited to ca. 90 °C by the durability of the membrane.

Previously, we have shown that the yield of CO_2 produced from ethanol oxidation can be greatly increased by pulsing the potential or current at the anode in order to promote the oxidation of adsorbed intermediates at a high potential and allow ethanol to adsorb and dissociate at a lower potential [22]. Ethanol vapor in a nitrogen stream was used as the fuel in order to achieve a rapid response in the analysis of CO_2 using a flow through non-dispersive infrared (NDIR) CO_2 detector. That work has been extended here to conditions more representative of a DEFC. Thus an aqueous ethanol solution (0.1 M) was feed to the anode, the cell was operated at temperatures up to 80 °C, and Pt and PtRu anode catalysts were compared. However, nitrogen was used at the cathode, rather than air, so that the anode potential could be more accurately controlled and CO_2 was not produced by the chemical reaction of ethanol with O_2 either at the cathode [23] or anode [24]. Under these conditions, the cathode acts as a dynamic hydrogen pseudo reference electrode (DHE). A previously reported experimental set-up [23] was modified as illustrated in Fig. 1. The CO_2 concentration in the combined anode and cathode exhausts was monitored so that the results were not impacted by crossover losses [23,25].

Potential cycling at a fixed sweep rate was employed here, rather than current or voltage pulses or ac perturbations, because this is a standard and widely used electroanalytical method. This provides more useful diagnostic information and allows comparisons with the extensive literature on ethanol voltammetry. The cell was operated with a dynamic hydrogen cathode (DHE) to provide a stable reference potential for the voltammetric (current vs. potential) measurements. The potential cycling results are compared with sweep and hold experiments in which a linear potential sweep was applied, and then the potential was held at the upper limit for the rest of the experiment. This mimics the initial forward scan in the corresponding cycling experiments, avoids the large current spike that accompanies a potential step, and represent constant potential behavior after the 30–80 s for the initial sweep.

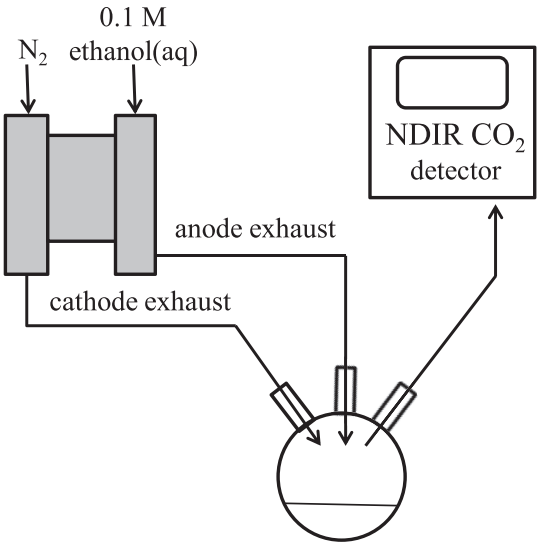

Fig. 1. Schematic diagram of the electrolysis cell and CO_2 analysis system.

The primary goals of this work were to determine whether the previously demonstrated strategy of adsorbing ethanol at low potentials and oxidatively stripping adsorbed intermediates (primarily CO) at higher potentials would be effective at higher potentials and with a PtRu anode catalyst, and to begin to explore how the efficiency of CO_2 production depends on the potentials employed. From a practical perspective, this knowledge could be used to improve the efficiency of DEFCs and ethanol electrolysis cells (EEC) which have recently been reported for producing clean hydrogen from ethanol [26]. Although, our experimental configuration is essentially an EEC, since H_2 is produced at the cathode, the dependence of CO_2 yields on anode potentials, temperature and catalyst should also provide a good guide to the behavior of a DEFC. Pulsed current, triangle, sawtooth, trapezoidal, and AC waveforms have been reported to prolonging the run time and life cycle of batteries [27], and pulsing has been used to improve the performance of methanol fuel cells [28] and CO tolerance of hydrogen fuel cells [29], and to decouple the parallel routes for the electrochemical oxidation of methanol [30]. Similar studies with DEFCs and EECs are therefore very pertinent.

2. Experimental

2.1. Chemicals and materials

Anhydrous ethanol (Commercial Alcohols Inc.) was used as received and double distilled water was used throughout all experiments. Cathodes and Pt anodes consisted of 4 mg cm^{-2} Pt black on Toray™ carbon fiber paper. PtRu anodes consisted of 5.5 mg cm^{-2} PtRu black on Toray™ carbon fiber paper. Nafion™ 115 membranes (Ion Power) were cleaned at 80 °C in 3% H_2O_2(aq) and 1 M H_2SO_4(aq), rinsed with water, and stored in water.

2.2. The cell

A 5 cm^2 commercial fuel cell (Fuel Cell Technology Inc.) was used. The anode inlet and outlet were both modified to prevent the ethanol solution from contacting any metal parts of the hardware. Membrane and electrode assemblies were prepared by pressing a 5 cm^2 anode and a 5 cm^2 cathode onto a Nafion™ 115 membrane in

the cell. The cell was operated with an anode feed of 0.10 mol L^{-1} ethanol solution at 0.69 mL min^{-1}. The cathode feed was N_2 at typically ca. 0.8 mL s^{-1}. The cell was operated with a Hokuto Denko HA-301 potentiostat and HB-104 function generator.

2.3. CO_2 analysis

Both the anode solution and the cathode gas (N_2) were passed into a 125 mL flask to collect the liquid. The N_2 stream exiting the flask was passed through a Telaire 7001 non-dispersive infrared CO_2 detector. The quantity of CO_2 detected over a specified period was calculated from the integral of the CO_2 concentration (ppm) readings (moles $CO_2 = \int(ppm_{CO_2} \cdot \dot{n}/10^6)dt$, where $\dot{n}$ is the N_2 flow rate in mol s^{-1}. The flow rate of N_2 reaching the detector was measure for each set of experiments and was typically ca. 0.8 mL s^{-1} (~3×10^{-5} mol s^{-1}). No corrections were made for the amount of CO_2 remaining in the liquid in the collection flask because based on Henry's Law they would be too small (ca. 2% or lower) to significantly influence the estimated CO_2 yields. However CO_2 retention does contribute to the slow response seen in the CO_2 concentration plots (see below).

The CO_2 detector was calibrated daily using CO_2 in N_2 standards prepared by injecting pure CO_2 in to an N_2 stream. The precision and accuracy of the system has been evaluated in a previous study, with relative standard deviations typically 5–10% at the CO_2 concentrations measured in this work [25]. The start times of the CO_2 traces reported here have been corrected for the minimum time required for the CO_2 to reach the detector. This causes the CO_2 collection time to be 50–100 s shorter than the cell run time.

3. Results and discussion

3.1. Potential cycling vs. fixed potential at ambient temperature

Figs. 2 and 3 illustrate how the current and production of CO_2 varied for two different potential waveforms, linear sweep with the potential held at the upper limit of 0.9 V, and potential cycling

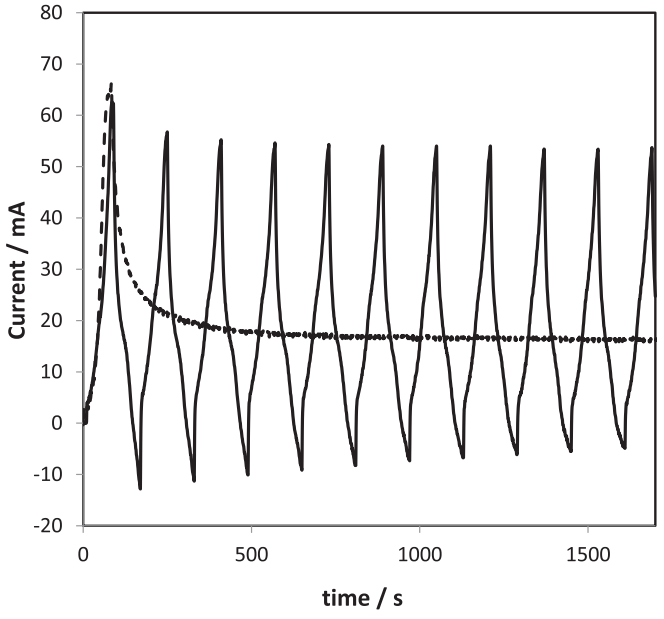

Fig. 2. Current vs. time plots for electrolysis of 0.1 M ethanol at ambient temperature at a Pt black anode using a linear potential sweep from 0.1 V vs. DHE with a potential hold at the upper limit of 0.9 V (dashed), and potential cycling between 0.1 and 0.9 V (solid). Sweep rate = 10 mV s^{-1}.

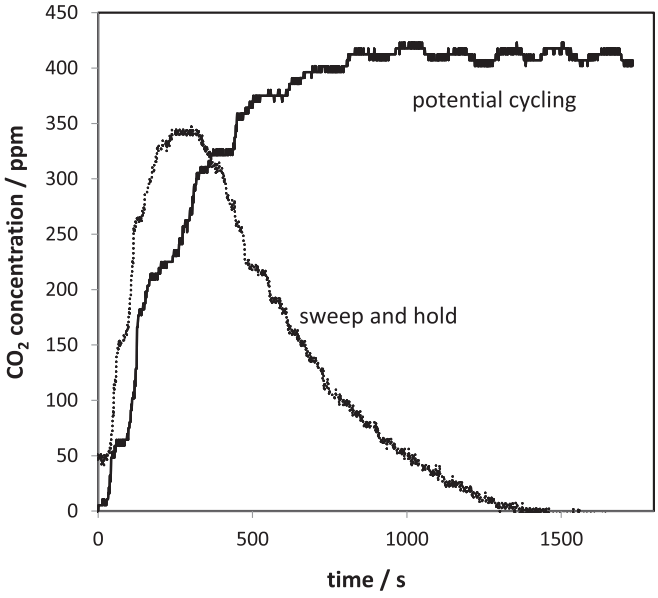

Fig. 3. CO_2 concentration vs. time plots for the electrolyses shown in Fig. 2. Data for sweep and hold (dotted) and potential cycling (solid) are shown. Lower potential = 0.1 V; upper potential = 0.9 V.

between 0.1 and 0.9 V. In both cases, the cell was operated for a total of 30 min. The sharp initial rise in the current in both experiments can be attributed mainly to the oxidation of adsorbed ethanol and partially oxidized intermediates (pre-adsorbed species) [31]. Since adsorbed CO is the primary intermediate, and the direct precursor to CO_2, all of the pre-adsorbed species are collectively referred to as CO_{ads} in this paper.

In the sweep and hold experiment, the current began to decay when the potential was held at 0.9 V, and reached an approximately steady value. In contrast, the current continued to be modulated in the potential cycling experiment, with the current decreasing during the reverse scans (0.9–0.1 V) and increasing on the forward scans (0.1–0.9 V). Apart from short periods at the end of each cycle due to discharging of the double layer (and possibly a small amount of methane production [16]), the current remained positive (oxidation of ethanol at the anode). The amplitude of the current response initially decreased with cycling, but then became reasonably steady.

As previously reported [22], the initial potential scan to 0.9 V produced a burst of CO_2 that can be attributed mainly to the oxidation of pre-adsorbed species (CO_{ads}). In the sweep and hold experiment, there was only transient CO_2 production, while cycling the potential continuously between 0.1 V and 0.9 V resulted in sustained CO_2 production. As previously reported for pulsed operation of a cell [22], the sustained CO_2 production in the potential cycling experiment can be attributed to the formation of a new layer of CO_{ads} at the lower potentials of each potential scan.

Analysis of the transient CO_2 response for the sweep and hold experiment provides important information on the response time of the CO_2 analysis system and the amount of CO_{ads}. Previous work with ethanol vapor indicated that the oxidation of CO_{ads} is much faster than the timescale in Fig. 3, as would be expected at 0.9 V. The breadth of the transient CO_2 response in Fig. 3 for the sweep and hold experiment can therefore be taken as representative of the signal broadening due to the flow and collection system used here to transfer the CO_2 produced by the cell from the liquid EtOH(aq) exhaust to the N_2 stream for analysis. Much faster responses can be achieved (e.g. 20 s [22]), but the system here was designed to

allow for long-term, high temperature operation of the cell with liquid EtOH(aq) rather than for a fast response.

Since the CO_2 reading dropped to zero in the sweep and hold experiment, it is a reasonable approximation to assume that most of the CO_2 produced in this experiment was due to the oxidation of CO_{ads}, and not from oxidation of ethanol diffusing to the electrode from the anode solution. Integration of this CO_2 transient provides the number of moles of CO_2 produced, 3.8 μmol, which should be a reasonable estimate of the number of moles of CO_{ads} (stripping of pure CO adsorbed on the type of anode used here produced ca. 6.2 μmol of CO_2, corresponding to an active Pt area of ca. 2500 cm^2).

The potential cycling experiment shown in Fig. 3 produced 11.3 μmol of CO_2. Of this, ca. 4 μmol would have been due to CO_{ads}, as in the sweep and hold experiment, leaving >7 μmol due to sustained ethanol oxidation. Since there may have also been some oxidation of ethanol from solution in the sweep and hold experiment, this is taken to represent a lower limit on the ethanol oxidized during the cycling experiment.

The important distinction that we are making here is between the oxidation of species already adsorbed on the electrode surface before the start of the experiment (i.e. CO_{ads}) and the oxidation of ethanol that diffuses to the electrode (from the solution) during the experiment. We have done this by showing that CO_2 production at constant potential is dominated by the former. This has very important implications in the determination of faradaic yields for ethanol oxidation, and the result at constant potential allows us to make a correction to account for the effects of the pre-adsorbed species.

Of central importance in the development of DEFC technology is the faradaic yield for CO_2 production (CO_2 yield), which is defined by Eq. (5).

$$CO_2\ \text{yield} = 6F\text{mol}_{CO_2}/Q \tag{5}$$

Here, mol_{CO_2} is the measured moles of CO_2 and Q is the charge passed by the cell. Application of this equation to the data from Figs. 2 and 3 produces apparent CO_2 yields of 6.1% and 21.6%, for the sweep and hold and potential cycling experiments, respectively. These are "apparent" yields because it is clear that much of the CO_2 is derived from CO_{ads} rather than ethanol from the solution, and so Eq. (5) is inaccurate in this situation. If all of the CO_2 was from CO_{ads} in the sweep and hold experiment, the actual CO_2 yield from ethanol would have been zero.

To obtain more accurate yields of CO_2 for the potential cycling experiment, corrections should be made to account for both the CO_2 produced from CO_{ads} (mol_{ads}) and the charge required to oxidize the CO_{ads} to CO_2, as shown in Eq. (6).

$$CO_2\ \text{yield} = 6F(\text{mol}_{CO_2} - \text{mol}_{ads})/(Q - n\text{Fmol}_{ads}) \tag{6}$$

Here, n is the average number of electrons required to produce CO_2 from the adsorbed species. It can range from 2 for adsorbed CO to 6 for adsorbed ethanol. The amount of CO_2 produced in the sweep and hold experiment is assumed to provide a reasonable estimate of mol_{ads}. Since the value of n is unknown, we report here the values for the two extremes, which are 14.7% for $n = 2$ and 15.5% for $n = 6$. These are average values for the whole 30 min experiment depicted in Figs. 2 and 3. However, it is clear from the comparison of the sweep and hold and cycling CO_2 profiles that the yield of CO_2 must have increased substantially over the first half of the cycling experiment. From an operational perspective, the sustained higher yield in the 2nd half of the experiment is more relevant. This can easily be estimated by applying Eq. (5) to the region of approximately steady state CO_2 production after ca. 900 s, where the effects of the transient CO_2 from CO_{ads} would have been minor. The CO_2 yield was thus calculated to be 26.5%, which should be a good estimate of the sustained production of CO_2 from ethanol being fed to the cell.

In considering which of the above methods is most appropriate for calculation of CO_2 yields, we must consider the origin of the adsorbates. When ethanol is introduced into the cell, it will spontaneously adsorb onto the Pt anode catalyst and there will be some electron transfer to the Pt as C–H and C–C bonds are spontaneously oxidized. A first step is illustrated by Eq. (7).

$$Pt + CH_3CH_2OH \rightarrow Pt{-}OCH_2CH_3 + e^- + H^+ \tag{7}$$

This reaction and parallel/subsequent oxidation steps will cause the anode open circuit potential to decrease and produce a variety of adsorbates in various oxidation states [32]. In addition, traces of oxygen in the system will contribute to the oxidation of the adsorbates without changing the anode potential. Since these processes result in partial oxidation of a substantial amount of ethanol without any charge being passed by the cell, including products from the adsorbates in the calculations of yields will produce large errors. These would be extremely difficult to accurately correct for, and so the most accurate approach is to apply Eq. (5) (and similar equations for other products) to data (charges and product amounts) collected after the products from the adsorbates have been flushed from the analysis system.

These results and considerations illustrate the complexities of trying to define and measure product yields from ethanol oxidation. Even with product collection over a 30 min period, the effects of pre-adsorbed intermediates are large, and many hours could be required to produce acceptable accuracy in some cases. The error can be minimized, however, by beginning product collection after a delay to avoid the collection of products from adsorbed species. An alternative method would be to carry out a pre-conditioning to remove (oxidize) the adsorbates. However, we have found this to be unsatisfactory because a fresh layer of adsorbates form when the cell is returned to the initial potential, or the anode is allowed to return to its open circuit potential. The charged passed during these processes would then have to be accounted for in determining the true CO_2 yield.

3.2. Effects of potential limits at ambient temperature

For most efficient operation of a DEFC, in addition to high levels of conversion of ethanol to CO_2, the cell potential should be as high as possible at the power output required for the application. In the experiments described here, the cell potential is the anode potential vs. DHE. Therefore low cell potentials in this work would correspond high efficiencies in a fuel cell and also in an ethanol electrolysis cell (EEC) producing hydrogen at the cathode [26].

The results in Fig. 3 show that CO_2 yields can be increased greatly and sustained by potential cycling, and this increases the chemical efficiency of the cell. In order to optimize the operation of either a DEFC or EEC, maximization of the yield of CO_2 should be balanced against minimizing the average anode potential and maximizing the power output of the cell (which increases with increasing anode potential to a certain point). To this end, experiments were run in potential cycling mode with various upper and lower limits (i.e. various average anode potentials and average power usage) to explore how the CO_2 yield depends on the voltage efficiency and power. The potential sweep rate was maintained at 10 mV s^{-1} for these experiments. Since long term performances are of interest here, CO_2 yields were determined by applying Eq. (5) to just the final 800 s of each experiment, although other parameters are reported for averages (current and power) or integrals (total CO_2) over the full duration of each experiment.

Table 1 summarizes results for a series of experiments in which the lower potential limit was set at 0.1 V while the upper limit was varied from 0.6 V to 0.9 V. The power can only be calculated for an EEC, since the cell was not operated as a fuel cell.

It is clear from the data in Table 1 that significant production of CO_2 from ethanol in solution can only be achieved with an upper potential of at least 0.8 V, and even then the CO_2 produced was found to decline (not shown) from a peak of 400 ppm at ca. 300 s to 240 ppm at 1700 s. It should be noted that the total CO_2 produced when the upper potential was 0.7 V was less than the CO_2 that could be produced from pre-adsorbed species (3.8 μmol), indicating that the actual CO_2 yield was much less than the value of 8.4% reported in Table 1. These results can be explained by the high potentials required to oxidize adsorbed CO. At Pt, this reaction occurs primarily over the range of ca. 0.6–0.8 V vs. RHE [33], which corresponds approximately with the observation of CO_2 evolution reported in Table 1.

From the data in Table 1 it can be shown, using Eq. (4), that increasing the upper potential from 0.8 V to 0.9 V increases the chemical efficiency by 5–11% depending on the CH_3CHO/CH_3CO_2H ratio. However, this is negated in the overall cell efficiency by the 14% increase in the average cell voltage required (or decreased cell voltage for a fuel cell). Nonetheless, this could still be of net benefit for an EEC because of the higher current and therefore higher rate of hydrogen production. This would not likely be the case for a DEFC, however, where the very low cell potential at the upper anode potential limit (if attainable) would lead to very low overall efficiencies.

Table 2 summarizes results for a series of experiments in which the upper potential limit was set at 0.9 V while the lower limit was varied from −0.2 V to +0.6 V. Although the use of negative potentials has little relevance to the operation of a fuel cell, it is relevant to an EEC where the anode could possibly be activated at such potentials. However, it can be seen from the results that low potentials were not beneficial, with CO_2 yields falling slightly for lower potential limits below 0.2 V and then sharply at −0.2 V. The lower yields in these cases may be due to adsorption of hydrogen atoms which can interfere with ethanol adsorption and dissociation. In light of these results, and the benefits of running the cell at high average current and power, the lower potential limit should be set to the highest value that does not compromise selectivity for the complete oxidation to CO_2. From the data in Table 2, this is 0.4 V (since the slightly higher yield at 0.1 V is within the experimental uncertainty). This potential is clearly sufficiently low for dissociative adsorption and oxidation of ethanol to occur on the time scale of the cycling, while 0.5 V is not low enough for these processes to occur efficiently.

3.3. Operation at elevated temperatures

Although the results presented in the previous sections are scientifically significant, the practical benefits of dissociative oxidation of ethanol to CO_2 at ambient temperature may be only minor. Of key technological importance is whether the benefits of potential cycling are maintained at the higher temperatures employed in applications, and whether lower anode potentials can be employed at higher temperatures. To explore this, experiments akin to those described above were run at 50 °C and 80 °C. The lower potential limit was maintained at 0.1 V in these experiments in order to allow comparison with the upper limit effects in Table 1, and to ensure that the lower potential did not begin to limit ethanol absorption when the sweep rate was increased.

Fig. 4 depicts apparent CO_2 yields vs. time for potential cycling between 0.1 V and 0.7 V at ambient temperature, 50 °C and 80 °C. These CO_2 yields were calculated by using Eq. (1) for each CO_2 ppm reading (converted to mol s^{-1}) and the average current (C s^{-1}) over the experiment. Although this results in significant errors in the actual yield at each point, it preserves the form of the CO_2 meter response (i.e. it provides a scaling of the CO_2 readings based on the charge passed at each temperature), which is informative.

An upper limit of 0.7 V was selected for Fig. 4 because it best illustrates the benefits of increasing the temperature. As seen in Table 1, an upper limit of 0.7 V was insufficient for complete

Table 1
Summary of data for the electrolysis of 0.1 M ethanol at ambient temperature at a Pt black anode under potential cycling conditions. The lower potential limit was 0.1 V.

Upper potential/V	Average current/mA	Total CO_2/μmol	Average CO_2 yield after 900 s	Average power[a]/mW
0.6	4.1	0	0	2.0
0.7	8.7	1.6	8.4%	4.9
0.8	13.4	9.1	21.3%	8.6
0.9	17.0	11.3	26.5%	11.6

[a] Power consumption for an EEC.

Table 2
Summary of data for the electrolysis of 0.1 M ethanol at ambient temperature at a Pt black anode under potential cycling conditions. The upper potential limit was 0.9 V.

Lower potential/V	Average current/mA	Total CO_2/μmol	Average CO_2 yield after 900 s	Average power[a]/mW
−0.2	14.6	2.6	6.6%	–
−0.1	16.5	7.4	14.7%	–
0	14.9	7.2	16.6%	10.1
0.1[b]	15.1	7.0	18.3%	10.3
0.2	16.3	8.6	21.2%	11.3
0.3	15.5	7.6	18.5%	10.7
0.4	18.4	9.3	19.9%	13.0
0.5	16.9	6.5	12.1%	12.3
0.6	16.3	1.8	1.9%	12.5

[a] Power consumption for an EEC. Not meaningful when negative cell potentials were employed.
[b] Values differ from those in Table 1 because this is a different data set for a different MEA.

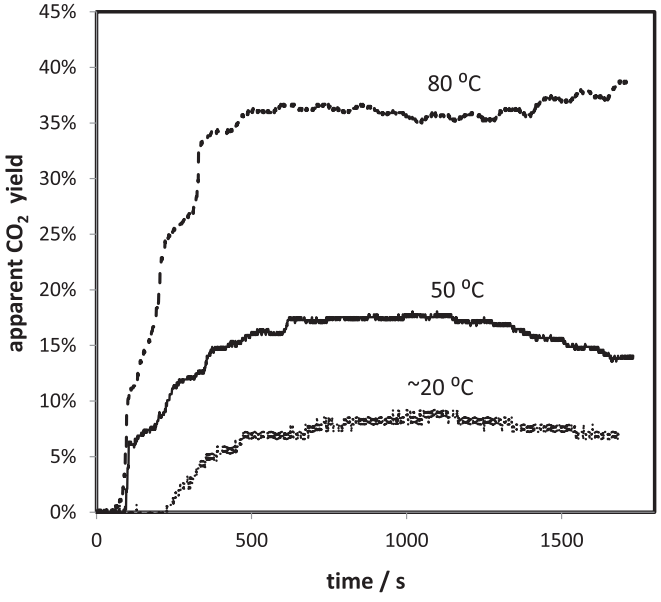

Fig. 4. Apparent CO_2 yields vs. time for electrolysis of 0.1 M ethanol at a Pt black anode during potential cycling between 0.1 V and 0.7 V at ambient temperature, 50 °C and 80 °C.

adsorbate removal at ambient temperature, resulting in a large drop in CO_2 yield relative to an upper limit of 0.8 V, and a decreasing yield at long times (Fig. 4). However, increasing the temperature resulted in large increases in CO_2 yield (Fig. 4) and at 80 °C the CO_2 production was sustained for the duration of the experiment. In addition, increasing the temperature increased the average currents and power greatly, and much more CO_2 was produced (Table 3).

Since complete oxidation of ethanol to CO_2 requires the cleavage of the strong C–C bond, higher temperatures generally increases CO_2 yields, and this has been well documented [15–21]. In addition, CO oxidation is promoted by higher temperature. Both of these effects are expected to decrease the benefits of potential cycling relative to its effects at ambient temperature. To explore this, potential cycling and sweep and hold experiments at 80 °C were compared (Table 4). At this temperature, a sweep rate of 100 mV s^{-1} during potential cycling was found to provide higher CO_2 yields than 10 mV s^{-1}, and so only the 100 mV s^{-1} data are reported here.

It is clear from the data in Table 4 that even at 80 °C higher CO_2 yields can be obtained at higher average currents when potential cycling is employed. The yield of 65% obtained for potential cycling is one of the highest reported for ethanol oxidation at 80 °C. For example, a value of 35% was measured by liquid chromatography for a DEFC with a Pt anode operated at 80 °C and a current density of 8 mA cm^{-2} [34], while a maximum of 50% at 70 °C was reported for a differential electrochemical mass spectrometry (DEMS) study of ethanol oxidation (0.1 M) at a gas diffusion electrode containing 4.3 mg cm^{-2} Pt black [16].

The decrease in yield seen in Table 4 as the potential was increased in the sweep and hold experiments is consistent with the trend reported in other studies [e.g. 18, 25], which is due to a decreasing tendency for C–C bond breaking and increasing oxygen coverage [18]. The opposite trend was observed from 0.6 to 0.8 V in the cycling experiments, which illustrates the benefits of using higher potentials to periodically strip adsorbates from the electrode.

3.4. PtRu anode catalyst

The results for cycling between 0.1 V and 0.8 V shown in Table 4 are attractive for operation of an EEC but not of practical value for a DEFC because the potential required to strip CO_{ads} from anode is too high to be produced by the cell. A Pt black anode catalyst was used in all experiments reported to this point. However, in practical applications, bi- or tri- metallic catalysts with higher activities and which can oxidize adsorbed CO at lower potentials are normally preferred [7,14]. PtRu was chosen here because it provides higher cell potentials than Pt in DEFCs, and allows adsorbed CO to be stripped at significantly lower potentials. It therefore offers the realistic possibility of increasing yields in a DEFC under potential cycling conditions. In addition, it should increase the efficiency of EECs.

Figs. 5 and 6 show current and CO_2 concentration traces for ethanol oxidation at 80 °C at a PtRu anode for cycling and sweep and hold experiments with an upper potential limit of 0.6 V. Average currents and CO_2 yields for these experiments and others with different upper potential limits are presented in Table 5. As expected [17,20], CO_2 yields were generally lower with the PtRu catalyst relative to Pt under the same conditions. However, higher currents were obtained at lower potentials, demonstrating the higher activity of PtRu for ethanol oxidation, and potential cycling was still very effective at increasing CO_2 yields. In addition, less positive upper anode potentials were required to obtain the benefits of cycling, as required for a DEFC. For example, cycling between 0.1 V and 0.6 V produced an average current of 110 mA, which was slightly higher than the 103 mA produced at a constant potential of 0.4 V, while the CO_2 yield during cycling was more than double (27.1%) that at constant potential (13.2%). The same cycling experiment with a Pt anode produced a higher CO_2 yield of 35.1% but a much lower average current of 28.4 mA (Table 4). These comparisons, and others based on the data in Tables 4 and 5 illustrate the trade-off required between efficiency (determined mainly by the anode potential and CO_2 yield) and power.

Table 3
Effects of temperature on cell performance parameters for the electrolysis of 0.1 M ethanol at ambient temperature at a Pt black anode for potential cycling between 0.1 V and 0.7 V at 10 mV s^{-1}.

Temperature/°C	Average current/mA	Total CO_2/μmol	Average CO_2 yield after 900 s	Average power[a]/mW
Ambient	8.7	1.6	8.4%	4.9
50	25.4	11.0	16.0%	14.6
80	50.8	48.2	31.9%	28.7

[a] Power consumption for an EEC.

Table 4
Average currents and CO_2 yields for the electrolysis of 0.1 M ethanol at 80 °C at a Pt black anode under sweep (10 mV s^{-1}) and hold, and potential cycling (100 mV s^{-1}) conditions. The lower potential limit was 0.1 V.

Upper potential/V	Average current after 900 s/mA		Average CO_2 yield after 900 s	
	Sweep and hold	Cycling	Sweep and hold	Cycling
0.4	21.4	–	45.6%	–
0.5	65.5	–	34.3%	–
0.6	83.5	28.4	33.5%	35.1%
0.7	82.5	53.1	28.4%	44.6%
0.8	69.9	82.7	23.2%	65.0%
0.9	74.9	121	11.9%	45.8%

– Results too uncertain to report.

4. Conclusions

Previous observations that potential modulation can increase the chemical efficiency of ethanol oxidation by promoting CO_2

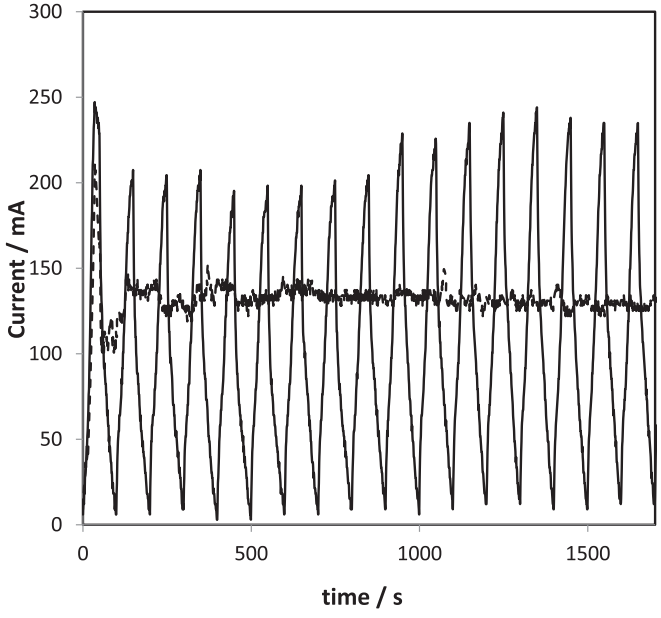

Fig. 5. Current vs. time plots for electrolysis of 0.1 M ethanol at 80 °C at a PtRu black anode using a linear potential sweep from 0.1 V vs. DHE with a potential hold at the upper limit of 0.6 V (dashed), and potential cycling between 0.1 and 0.6 V (solid). Sweep rate = 10 mV s^{-1}.

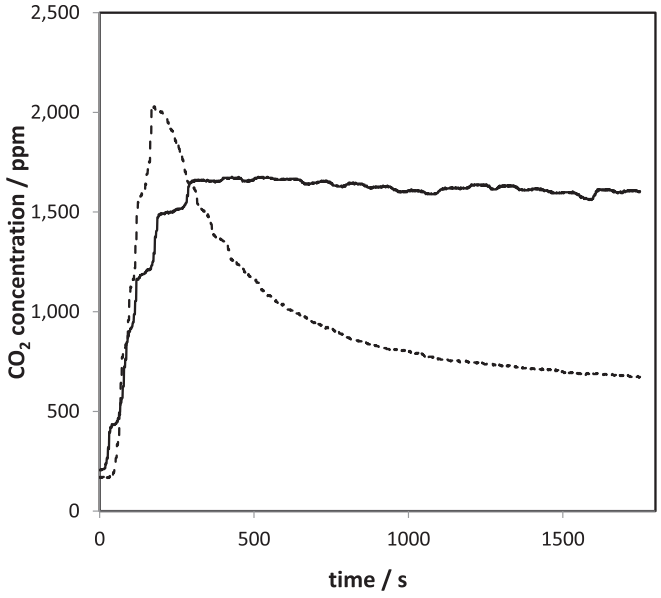

Fig. 6. CO_2 concentration vs. time plots for the electrolyses shown in Fig. 5. Data for sweep and hold (dashed) and potential cycling (solid) are shown. Lower potential = 0.1 V; upper potential = 0.6 V.

Table 5
Average currents and CO_2 yields for the electrolysis of 0.1 M ethanol at 80 °C at a PtRu black anode under sweep (10 mV s^{-1}) and hold, and potential cycling (10 mV s^{-1}) conditions. The lower potential limit was 0.1 V.

Upper potential/V	Average current after 900 s/mA		Average CO_2 yield after 900 s	
	Sweep and hold	Cycling	Sweep and hold	Cycling
0.4	103	34.4	13.2%	17.3%
0.5	133	73.3	13.2%	23.3%
0.6	131	110	11.2%	27.1%
0.7	121	111	7.8%	32.4%
0.8	132	130	4.6%	28.3%

production have been extended to the electrolysis of ethanol in aqueous solution. The effects of potential limits, temperature and Pt vs. PtRu anode catalysts have been explored. In all cases, cycling the potential has been shown to increase the yield of CO_2 and in many cases the effects are substantial. For example, at ambient temperature with a Pt anode the yield has been increased from <<6.4% to 26%, while a yield of 65% has been achieved at 80 °C. PtRu provides lower CO_2 yields than Pt, but significantly decreases the anode potential required. At 80 °C a maximum yield of 32.4% was obtained under cycling conditions, while the best yield at constant potential was only 13.2%.

These results demonstrate how the efficiency of direct ethanol fuel cells and ethanol electrolysis cells can be improved by employing potential modulation techniques. It can be anticipated that further optimization of the operational parameters (potential waveform and limits, sweep rate, temperature) will lead to higher efficiencies, and that efficient oxidation of ethanol can be sustained indefinitely.

Acknowledgments

This work was supported by the Natural Sciences and Engineering Research Council of Canada and Memorial University.

References

[1] F. Vigier, S. Rousseau, C. Coutanceau, J.M. Leger, C. Lamy, Top. Catal. 40 (2006) 111.
[2] U.B. Demirci, J. Power Sources 169 (2007) 239.
[3] X.L. Li, A. Faghri, J. Power Sources 226 (2013) 223.
[4] A. Brouzgou, A. Podias, P. Tsiakaras, J. Appl. Electrochem. 43 (2013) 119.
[5] B. Braunchweig, D. Hibbitts, M. Neurock, A. Wieckowski, Catal. Today 202 (2013) 197.
[6] M.Z.F. Kamarudin, S.K. Kamarudin, M.S. Masdar, W.R.W. Daud, Int. J. Hydrogen Energy 38 (2013) 9438.
[7] J. Friedl, U. Stimming, Electrochim. Acta 101 (2013) 41.
[8] F. Vigier, C. Coutanceau, A. Perrard, E.M. Belgsir, C. Lamy, J. Appl. Electrochem. 34 (2004) 439.
[9] R.B. Kutz, B. Braunschweig, P. Mukherjee, R.L. Behrens, D.D. Dlott, A. Wieckowski, J. Catal. 278 (2011) 181.
[10] S.E. Evarts, I. Kendrick, B.L. Wallstrom, T. Mion, M. Abedi, N. Dimakis, E.S. Smotkin, ACS Catal. 2 (2012) 701.
[11] R. Kavanagh, X.M. Cao, W.F. Lin, C. Hardacre, P. Hu, J. Phys. Chem. C 116 (2012) 7185.
[12] J. Melke, A. Schoekel, D. Gerteisen, D. Dixon, F. Ettingshausen, C. Cremers, C. Roth, D.E. Ramaker, J. Phys. Chem. C 116 (2012) 2838.
[13] J.F. Gomes, K. Bergamaski, M.F.S. Pinto, P.B. Miranda, J. Catal. 302 (2013) 67.
[14] E. Antolini, J. Power Sources 170 (2007) 1.
[15] A.S. Arico, P. Creti, P.L. Antonucci, V. Antonucci, Electrochem. Solid State Lett. 1 (1998) 66.
[16] V. Rao, C. Cremers, U. Stimming, L. Cao, S.G. Sun, S.Y. Yan, G.Q. Sun, Q. Xin, J. Electrochem. Soc. 154 (2007) B1138.
[17] A. Ghumman, G. Li, D.V. Bennett, P.G. Pickup, J. Power Sources 194 (2009) 286.
[18] S. Sun, M.C. Halseid, M. Heinen, Z. Jusys, R.J. Behm, J. Power Sources 190 (2009) 2.
[19] D.A. Cantane, W.F. Ambrosio, M. Chatenet, F.H.B. Lima, J. Electroanal. Chem. 681 (2012) 56.
[20] J.J. Linares, S.C. Zignani, T.A. Rocha, E.R. Gonzalez, J. Appl. Electrochem. 43 (2013) 147.
[21] J. Seweryn, A. Lewera, Appl. Catal. B 144 (2014) 129.
[22] A. Ghumman, P.G. Pickup, J. Power Sources 179 (2008) 280.
[23] D.D. James, P.G. Pickup, Electrochim. Acta 55 (2010) 3824.
[24] A. Jablonski, P.J. Kulesza, A. Lewera, J. Power Sources 196 (2011) 4714.
[25] D.D. James, P.G. Pickup, Electrochim. Acta 78 (2012) 274.
[26] C. Lamy, T. Jaubert, S. Baranton, C. Coutanceau, J. Power Sources 245 (2014) 927.
[27] L.R. Chen, J.J. Chen, C.M. Ho, S.L. Wu, D.T. Shieh, IEEE Trans. Ind. Electron. 60 (2013) 5620.
[28] M. Neergat, T. Seiler, E.R. Savinova, U. Stimming, J. Electrochem. Soc. 153 (2006) A997.
[29] L.P.L. Carrette, K.A. Friedrich, M. Huber, U. Stimming, Phys. Chem. Chem. Phys. 3 (2001) 320.
[30] R. Nagao, D.A. Cantane, F.H.B. Lima, H. Varela, Phys. Chem. Chem. Phys. 14 (2012) 8294.
[31] H. Wang, Z. Jusys, R.J. Behm, J. Phys. Chem. B 108 (2004) 19413.
[32] J.M. Leger, J. Appl. Electrochem. 31 (2001) 767.
[33] P. Urchaga, S. Baranton, C. Coutanceau, G. Jerkiewicz, Langmuir 28 (2012) 3658.
[34] S. Rousseau, C. Coutanceau, C. Lamy, J.M. Leger, J. Power Sources 158 (2006) 18.